LANGMUIR

Interfaces: Adsorption, Reactions, Films, Forces, Measurement Techniques, Charge Transfer, Electrochemistry, Electrocatalysis, Energy Production and Storage

Bis (tri-alkylsilyl oxide) silicon phthalocyanines: understanding the role of solubility on device performance as ternary additives in organic photovoltaics

Mario C. Vebber, Trevor M. Grant, Jaclyn L. Brusso, and Benoît H. Lessard

Langmuir, **Just Accepted Manuscript** • DOI: 10.1021/acs.langmuir.9b03772 • Publication Date (Web): 24 Feb 2020

Just Accepted

is published by the American Chemical Society. 1155 Sixteenth Street N.W., Washington, DC 20036

Bis (tri-alkylsilyl oxide) silicon phthalocyanines: understanding the role of solubility on device performance as ternary additives in organic photovoltaics.

Mário C. Vebber[1], Trevor M. Grant[1], Jaclyn Brusso[2] and Benoît H. Lessard[1]*

[1]Department of Biological and Chemical Engineering, University of Ottawa, 161 Louis Pasteur, Ottawa, Ontario K1N 6N5, Canada

[2]Department of Chemistry and Biomolecular Sciences, University of Ottawa, 150 Louis Pasteur, Ottawa, Ontario K1N 6N5, Canada;

[*]Author to whom correspondence should be addressed: benoit.lessard@uottawa.ca

Keywords: organic photovoltaics, ternary additive, phthalocyanine, solubility.

Abstract

The use of ternary additives in organic photovoltaics (OPV) is a promising route to improve overall device performance. Silicon phthalocyanines (SiPcs) are ideal candidates due to their absorption profile, low cost and ease of synthesis and chemical tunability. However, to date only a few examples have been reported and specific strategies to help design improved ternary additives have not been established. In this study, we report a relationship between ternary additive solubility and device performance, demonstrating that device performance is maximized when the SiPc additive solubility is similar to that of the donor polymer (P3HT, in this case). This improved performance can be attributed to the favored interfacial precipitation of the SiPcs when its solubility matches that of the other components of the thin film. The power conversion efficiency (PCE) varied from 2.4% to 3.4% by using axially substituted SiPcs with different solubilities, where the best ternary additive led to a 25% increase in PCE compared to the baseline device.

Introduction

Organic photovoltaics (OPVs) are an emerging solar energy technology, presenting a number of advantages over their inorganic counterparts, such as low manufacturing

cost, ease of integration onto flexible substrates, mechanical robustness and recyclability.[1–4] Recently, single-junction OPVs, on a laboratory scale, achieved record power conversion efficiency (PCE) between 15-17%.[5,6] As OPV performance continues to rise and with the promise of high throughput manufacturing, it is predicted that their price will plunge below that of conventional inorganic cells.[7]

One of the main challenges with bulk heterojunction (BHJ) OPVs is to maximize light harvesting across the visible and near-infrared regions of the solar spectrum as most organic compounds tend to demonstrate a relatively narrow absorption band in the visible spectrum.[8,9] The addition of a photosensitizing ternary additive to the donor/acceptor blend is a straightforward approach to increase the overall absorption of the active layer. Secondary functionality of these additives can also be achieved such as enhancement of the film microstructure,[10,11] favoring phase separation in the nanoscale, and compatibilization of energy levels between donor and acceptor,[12] which can increase charge separation and even enhance device stability, through the use of crosslinking groups.[13,14]

One class of materials that has been widely used for application in electronic devices are metal/metalloid containing phthalocyanines (MPcs). While divalent MPcs (Zn, Cu,

etc) are widely reported in the literature as active materials, tetravalent MPcs are less studied. Tetravalent MPcs, such as silicon phthalocyanines (SiPcs), have two axial bonds available for chemical modification, imparting broader chemical versatility and facilitating the relatively easy tuning of electronic and physical properties.[15–18] MPcs have also demonstrated the ability to act as non-fullerene electron acceptors in bulk heterojunction (BHJ) OPVs.[18] Furthermore, these dyes have found application as commercial photoreceptors for almost 50 years and, prior to that, as a commercial pigment.[15] The chemistry and purification of MPcs is relatively simple and straightforward compared to conventional organic semiconductors, making them desirable candidates for commercially viable OPV devices.[15–18] SiPcs have a high molar extinction coefficient and absorb light in the near infrared region, complimenting well-established donor/acceptor pairs, such as poly-3-hexylthiophene (P3HT) and phenyl-C_{61}-butyric-acid-methyl-ester (PCBM), that often show poor performance in that region of the solar spectrum.[13,18,19]

Honda *et al.* first reported the use of bis(trihexyl)silyl oxide SiPc as an additive in a P3HT / $PC_{61}BM$ BHJ OPV and obtained a 50% increase in current density (J_{sc}) .[20,21] The same group also found that the SiPc derivative had a high performance as an

additive in OPVs due to their tendency to migrate to the donor-acceptor interface, where they improve charge collection and charge transfer between the donor and the acceptor.[22] Silicon napthalocyanines (SiNcs) have also been applied in OPVs, with similar increases in J_{sc}, by harvesting near infra-red light.[23] Alternatively, Ke *et al.* functionalized SiPcs with pyrenes in the axial position, resulting in effective ternary additives with increased absorption range, which were reported to increase J_{sc} by 20% and PCE by 50%. [24] It has been demonstrated that the absorption coverage can be further improved by a combination of different SiPcs and SiNcs as ternary and quaternary additives.[20,25] Moreover, SiPc derivatives have also been applied in light-emitting diodes (OLEDs) [26–28] and in organic thin film transistors (OTFTs).[29–33].

While most reports focus on energy level tuning of ternary additive materials, less attention is given to the role of other physical properties, such as solubility and crystal structure.[6,34] In the case of SiPcs, it has been shown that axial functionalization has little to no effect on the frontier orbital energy levels or optical properties; however, it does lead to significant effects in molecular packing.[16,35]

The solubility of active materials is often analyzed in the search for greener solvents, yet studies focused on the relationship between solubility and the performance of the

resulting devices are surprisingly scarce, especially given the interest in solution processable OPVs.[36,37] Troshin *et al.* have demonstrated that the solubility of fullerene acceptors significantly impacts the PCE of P3HT:fullerene devices, and that best performance is achieved when the solubility of the fullerene acceptor is close to that of P3HT, leading to favorable nanomorphology.[38] However, no similar studies have been performed on ternary additives. To that end, we present herein the synthesis and characterization of nine different SiPcs functionalized with a range of axial silanes, and their employment as additives in P3HT / $PC_{61}BM$ BHJ OPVs. This study demonstrates that a small change in structure has a significant effect on the solubility and, ultimately, the performance of the resulting ternary BHJ/OPV devices. This investigation therefore represents the first report that facilitates the establishment of new design rules for ternary additives.

Experimental Section

Materials

N-butyldimethylchlorosilane (>95%), hexyldimethylchlorosilane (>95%), n-octyldimethylchlorosilane (>95%), n-dodecyldimethylchlorosilane (>95%), tri-n-

ethylchlorosilane (>95%), tri-n-butylchlorosilane (>95%), tri-n-hexylchlorosilane (>95%) and n-octyldiisopropylchlorosilane (>95%) were purchased from Gelest and used as received. P3HT (MW = 75 kDa, 96% regioregular) was purchased from Rieke Metals and $PC_{61}BM$ from Nano-C, respectively. All solvents were purchased from commercial suppliers and used without further purification. Dichlorosilicon phthalocyanine (Cl_2-SiPc) [39] was synthesized according to reported procedures in the literature.

Synthesis of silicon phthalocyanine ternary additives

The general synthetic procedure for SiPc axial functionalization was performed as follows [40]: Cl_2-SiPc (1.6 mmol), sodium hydroxide (8.6 mmol), trialkylchlorosilane (6 mmol), Aliquat HTA-1 (0.015 g) and chlorobenzene (10 ml) were added to a 100 ml flask and were stirred under reflux (132 °C). After 1 h, additional trialkylchlorosilane (1.9 mmol) was added to the reaction medium, which was left stirring at reflux for another hour. At this point, additional sodium hydroxide (3.4 mmol) and trialkylchlorosilane (1.9 mmol) were added to the mixture and refluxed for further 4 h before removing from heat. The dark-blue solution was then filtered to remove a purple

residue, and the solvent was removed under reduced pressure. Methanol was added to the resulting residue affording the desired product, which was isolated upon filtration, washed with methanol and dried in a vacuum oven. Purification was carried out by train sublimation (180 °C to 250 °C, 130 mTorr) before their application in OPVs. Using this procedure, the soluble X_2-SiPcs shown in Fig. 1 were produced:

(1) Bis(thexyldimethylsilyl oxide) silicon phthalocyanine: ^{1}H NMR 9.60 – 9.66 (m, 8 H), 8.28 – 8.34 (m, 8H), -0.95 – -1.0 (m, 2 H), -1.0 – -1.05 (d, 12 H) and -1.52 – -1.44 ppm

(s, 12 H). ^{13}C NMR 148 , 136 , 130 , 123 (Aromatic); 32 , 22 , 17 , 16 and -5 ppm (Alkyl). MS (EI) expected mass: 858.37, obtained mass: 858.3. Yield: 0.45 g (30%).

(2) Bis(n-octyldimethylsilyl oxide) silicon phthalocyanine: ^{1}H NMR 9.60 – 9.66 (m, 8 H), 8.28 – 8.34 (m, 8H), 1.11 – 1.27 (m, 4 H), 0.92 – 1.04 (m, 4 H), 0.85 – 0.94 (t, 6H), 0.68 – 0.80 (m, 4H), 0.25 – 0.37 (m, 4H), -0.23 – -0.10 (m, 4H) and -1.17 – -1.04 ppm (m, 4H). ^{13}C NMR 148 , 136 , 130 , 123 (Aromatic); 32 (2), 29 , 23 , 21 , 15 , 14 n, -4 ppm (Alkyl). MS (EI) expected mass: 914.43, obtained mass: 914.4. Yield: 0.45 g (30%).

(3) Bis(n-dodecyldimethylsilyl oxide) silicon phthalocyanine: ^{1}H NMR 9.60 – 9.66 (m, 8 H), 8.28 – 8.34 (m, 8H), 1.20 – 1.39 (m, 20 H), 1.10 – 1.19 (m, 4 H), 0.95 – 1.02 (m, 4H), 0.88 – 0.95 (t, 6H), 0.64 – 0.73 (m, 4H), 0.19 – 0.31 (m, 4H), -0.29 – -0.18 (m, 4H) and -1.42 – -1.31 ppm (m, 4H). ^{13}C NMR 148 , 136 , 130 , 123 (Aromatic); 32 (2), 29 (5), 23 , 21 , 15 , 14 n, -4 ppm (Alkyl). MS (EI) expected mass: 1026.56, obtained mass: 1026.5. Yield: 0.50 g (28%).

(4) Bis(tri-n-ethyl oxide) silicon phthalocyanine: ^{1}H NMR 9.60 – 9.66 (m, 8 H), 8.28 – 8.34 (m, 8H) and -1.30 – -1.20 ppm (t, 12 H). ^{13}C NMR 148 , 136 , 130 , 123 (Aromatic); 5 and 3 ppm (Alkyl). MS (EI) expected mass: 802.31, obtained mass: 802.3. Yield: 0.28 g (20%).

(5) Bis(triisobutylsilyl oxide) silicon phthalocyanine: ^{1}H NMR 9.60 – 9.66 (m, 8 H), 8.28 – 8.34 (m, 8H), -0.58 – -0.50 (d, 12H) and -0.96 – -0.85 ppm (m, 2H). ^{13}C NMR 148 , 136 , 130 , 123 (Aromatic); 25 , 24 and 22 ppm (Alkyl). MS (EI) expected mass: 970.49, obtained mass: 970.5. Yield: 0.49 g (30%).

(6) Bis(tri-n-butylsilyl oxide) silicon phthalocyanine: ^{1}H NMR 9.60 – 9.66 (m, 8 H), 8.28 – 8.34 (m, 8H), -0.12 – 0.12 (m, 30H) and -1.36 – -1.22 ppm (m, 12H). Yield:

0.52g (30%).

^{13}C NMR and mass spec are published elsewhere. [18]

(7) Bis(tri-n-hexylsilyl oxide) silicon phthalocyanine: ^{1}H NMR 9.60 – 9.66 (m, 8 H), 8.28 – 8.34 (m, 8H), 0.73 – 0.91 (m, 12H), 0.61 – 0.74 (t, 18H), 0.28 – 0.42 (m, 12H), -0.12 – 0.06 (m, 12H) and -1.38 – -1.22 ppm (m, 12H). Yield: 0.60g (31%).^{13}C NMR and mass spec are published elsewhere. [41]

(8) Bis(diisopropyloctylsilyl oxide) silicon phthalocyanine: ^{1}H NMR 9.60 – 9.66 (m, 8 H), 8.28 – 8.34 (m, 8H), 1.16 to 1.31 (m, 4H), 1.01 to 1.14 (m, 4 H), 0.77 to 0.95 (m, 8H), 0.33 to 0.45 (m, 4H), 0.05 to 0.22 (m, 4H), -1.05 to -0.90 (m, 4H) and -1.40 to -1.20 (m, 20H) and -2.10 to -2.00 ppm (m, 2H). ^{13}C NMR 148, 136, 130, 123 (Aromatic); 33 , 32, 29, 28, 22, 21, 15, 14, 11 and 10 ppm (Alkyl). MS (EI) expected mass: 1026.56, obtained mass: 1026.5. Yield: 0.28 g (17%).

(9) Bis(n-butyldimethyl oxide) silicon phthalocyanine: No appreciable amount of this compound was obtained.

Mass obtained from MS was defined according to the fragment corresponding to the entire molecule.

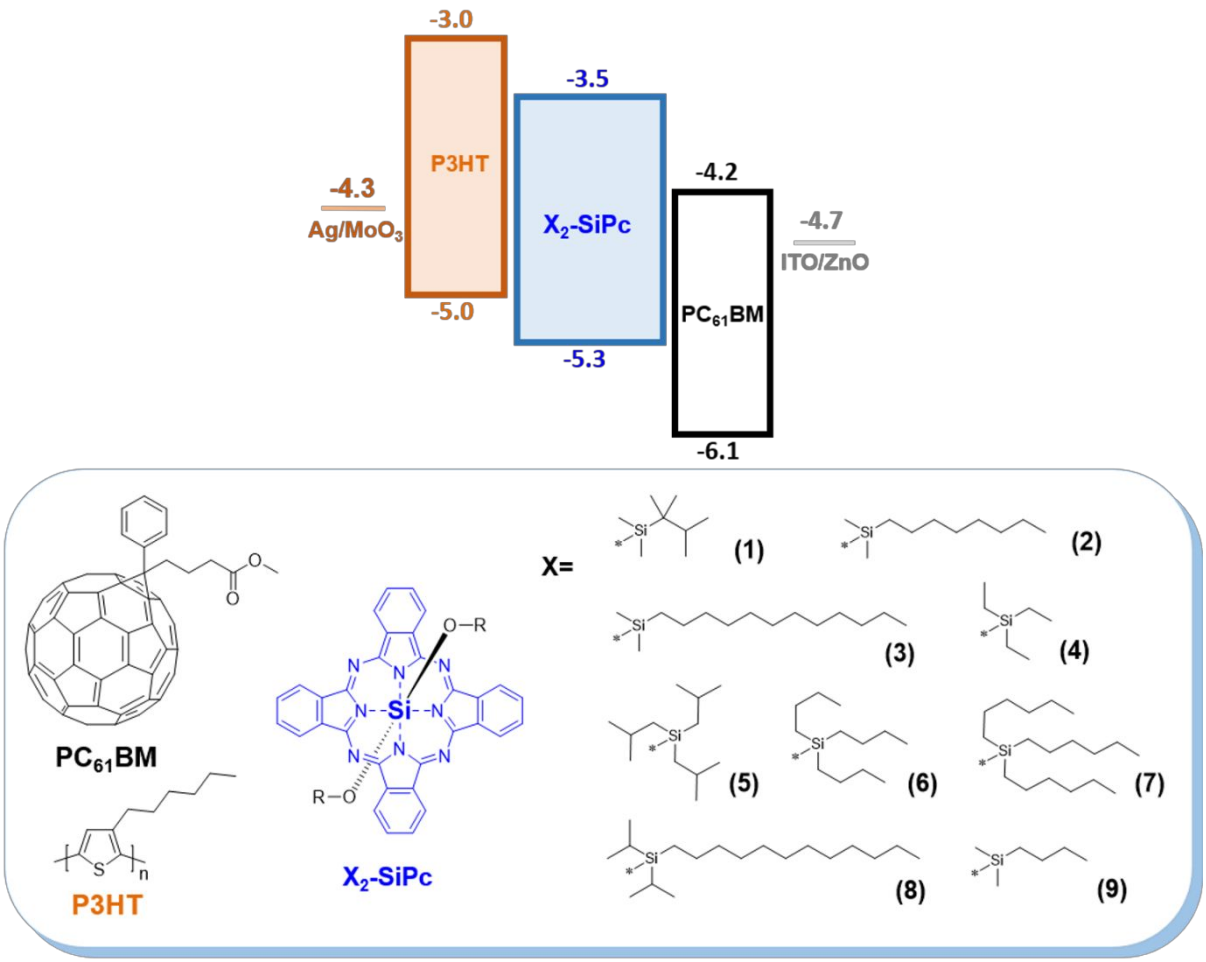

Figure 1. Axially substituted X_2-SiPcs synthesized and characterized in the present study.

Materials Characterizations

^{1}H NMR spectra were obtained on a Bruker Avance II spectrometer in $CDCl_3$ and operating frequency of 400 MHz. Molecular absorption spectra in the ultraviolet and visible regions (UV-Vis) were recorded on an Ocean Optics Flame spectrophotometer, using a DH-2000 light source and a quartz cuvette with a path length of 10 mm. Cyclic

voltammograms were obtained using a VersaSTAT 3 potentiostat, a polished platinum disk as working electrode, a coiled platinum wire as counter electrode, and an Ag/AgCl electrode as reference. Three cycles from 0 V to 1.6 V were recorded at a scan rate of 0.1 V/s. Such experiments were carried out in dichloromethane (DCM) solutions with tetrabutylammonium perchlorate as the supporting electrolyte. Highest occupied molecular orbital (HOMO) energy levels were estimated according to the empirical correlation E_{HOMO} (eV) = -($E_{ox,onset}$ - $_{Eox\ Fc/Fc+,onset}$) - 4.80 eV, where $E_{ox,onset}$ and $E_{oxFc/Fc+,onset}$ are the onset oxidation potentials of the sample and of the ferrocene standard, respectively. Solubility measurements were conducted by mixing 10, 20 or 40 mg of the axially substituted SiPcs in 0.15 ml of 1,2-dichlorobenzene and stirring the mixture for 1 h at 70°C, before allowing these mixtures to cool down to room temperature. The samples were then filtered through a 0.25 µm Teflon syringe filter and 100 µL samples of filtrate were collected, dried at 150°C under vaccum for 2 h and then weighted to calculate the solubility.

Device Preparation

The OPV devices were fabricated on indium tin oxide (ITO) coated glass slides (1 in x 1 in), which were cleaned in an ultrasonic bath with soapy water, deionized water, acetone then methanol, before being treated with air plasma for 15 min. 150 uL of a zinc solution constituted of zinc acetate (0.195 g), ethanolamine (0.055 ml) and ethanol (6 ml) was spincoated on the ITO substrate at 2000 RPM for 1 min. These films were annealed at 180°C for 1 h, leading to the formation of the ZnO electron transport layer. The active layer solutions were prepared by dissolving P3HT and $PC_{61}BM$ in DCB at a 1:0.8 ratio. Different amounts of X_2-SiPcs were added to the aforementioned mixture to form solutions with P3HT concentration of 20 mg ml^{-1} and additive ratios of 2.7 wt %, 3.7 wt % and 4.8 wt %. These solutions were spincoated at 1000 RPM, for 35s inside a N_2 glovebox. The films were dried at room temperature, open to the glovebox atmosphere. Finally, the devices were moved into an evaporator chamber where MoO_3 (7 nm) and Ag (70 nm) films were evaporated at a pressure of 10^{-6} torr to make 5 devices per substrate, with areas of 0.32 cm^2, as defined by shadow masks. The device structure and its components' energy levels are depicted in Fig. 1. Current density vs. voltage curves were obtained with a Kiethley 2400 equipment, under 1000 W m^{-2} illumination from an AM1.5 xenon lamp solar simulator, inside a

glovebox. Devices were encapsulated using an optical adhesive (Norland NOA61), which was cured under an UV lamp (6 W), and a glass coverslip before EQE measurements in air, in a Newport Quantx-300 equipment.

Results and Discussion

Synthesis and Characterization of SiPcs

The X_2-SiPcs described here were all synthesized using the same experimental procedure, in which various trialkylchlorosilanes were used to afford the nine different derivatives outlined in Fig. 1. The overall yields from diiminoisoindoline to axially substituted SiPcs varied from 20 to 40% by weight (see Experimental Section for details). The reactions affording the lowest yields were associated with low MW silanes, such as (4) and (9), which may be attributed to the preferential formation of siloxane (i.e., R–O-Si-O–R) byproducts. In fact, this reoccurring impurity may be present even after sublimation, which can be seen in the ^{1}H NMR spectrum as a strong singlet with a chemical shift of approximately 0.5 ppm (see ESI figures S1-S19 for NMR). Nonetheless, running the sublimation overnight or washing the solids with hexanes are both effective ways to remove this impurity. Unfortunately, no appreciable

amounts of compound (9) were obtained due to the formation of this byproduct, which inhibited its incorporation into devices or further characterization. Nevertheless, this is a simple and straightforward method to obtain various X_2-SiPcs that does not require dry solvents or oxygen free environments.

UV-Vis Spectroscopy and Cyclic Voltammetry

The eight X_2-SiPc compounds were characterized optically and electrochemically to estimate their optical bandgap (E_g), highest occupied molecular orbital energy levels (E_{HOMO}) and lowest unoccupied molecular orbital energy levels, E_{LUMO} (Table 1).

Table 1. Optical and electrochemical (CV) characterization of silicon phthalocyanine derivatives

Compound	λ_{max} a)	E_g a)	E_{Ox} b)	E_{HOMO} c)	E_{LUMO} c)
(1)	671	1.81	0.98	-5.31	-3.50
(2)	672	1.80	0.96	-5.29	-3.49
(3)	670	1.81	0.96	-5.29	-3.48
(4)	671	1.81	0.97	-5.30	-3.49

(5)	672	1.81	0.95	-5.28	-3.47
(6) [18]	669	1.82	0.98	-5.31	-3.49
(7) [18]	669	1.82	0.98	-5.31	-3.49
(8)	672	1.81	0.95	-5.28	-3.47

[a)] peak absorbance determined in DCM solution, E_g = energy bandgap determined from the onset of UV-Vis absorption spectrum.

[b)] half wave potential of oxidation measured using an Ag/AgCl reference electrode and platinum rod working electrode in DCM solution. [c)] E_{HOMO} = highest occupied molecular orbital energy level determined using the empirical correlation E_{HOMO} (eV) = $-(E_{ox,onset} - E_{ox\ Fc/Fc+,onset}) - 4.80$. Lowest unoccupied molecular orbital energy level calculated from $E_{LUMO} = E_{HOMO} + E_g$.

As expected, all SiPc derivatives have effectively the same energy levels and optical bandgap. The UV-Vis and CV spectra are presented in Fig. 2, except for compounds (6) and (7), which have been published elsewhere.[18] These values are identical to our previously published bis(tri-n-hexylsilyl) SiPc and bis(tri-n-butylsilyl) SiPc derivates (6 and 7 from Fig. 1).[18] For the current study these results indicate that the axial substituents have no effect on the absorption profiles, or frontier molecular orbitals, which is key when comparing their performance in OPVs with respect to their physical properties, such as solubility.

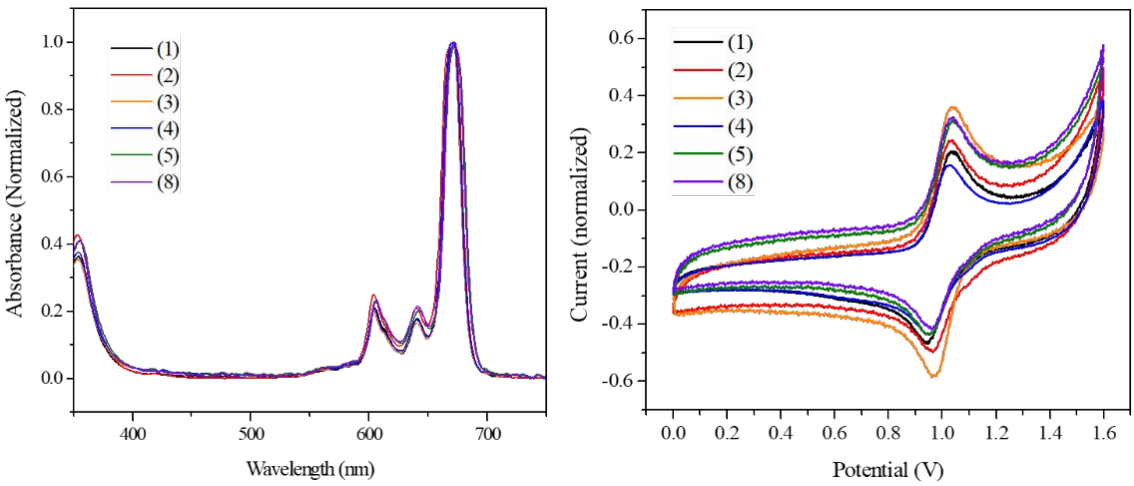

Figure 2. a) UV-Vis spectrum of the X_2-SiPcs and b) CV spectra and X_2-SiPcs for HOMO level estimation.

Solubility

The solubility of P3HT, $PC_{61}BM$ and all eight X_2-SiPcs was determined in dichlorobenzene (see experimental section for details) and plotted in Fig. 3. It is clear that small changes in the alkylsilanes functional groups leads to a large difference in the solubility of the compounds, which varies from 8 to 190 mg mL^{-1}. It would appear that an increase in roughly one order of magnitude in solubility was observed for SiPc derivatives with alkyl chains going from 6 to 8 carbons (Fig. 3). This type of significant increase in solubility has been observed in other small molecules such as fullerenes for example, where changing the alkyl solubilizing group from ethyl to butyl, increases the solubility from <1 mg ml^{-1} to >70 mg ml^{-1}.[38] Unsubstituted SiPcs are very insoluble due to strong π-π

intramolecular interactions. Since the SiPc radius (0.86 nm) [15] is roughly equivalent to the length of a hexyl group (0.82 nm), one can hypothesize that alkyl groups longer than 6 carbons in the axial position will efficiently disrupt ring-ring interactions and cause the observed jump in solubility.

P3HT and $PC_{61}BM$ were characterized to have a solubility of 100 and 140 mg mL^{-1}, respectively. It is important to note that the previously reported solubilities for $PC_{61}BM$ and P3HT are within 50 to 80 mg mL^{-1},[38] which are obtained by UV-Vis absorption spectroscopy. Nevertheless, all solubilities in this study were measured with the same procedure to ensure reliable comparisons can be made. These results further suggest that the changes in axial silane groups on the SiPcs has little to no effect on optical, electrochemical or hydrophobicity properties but has a significant impact on the solubility.

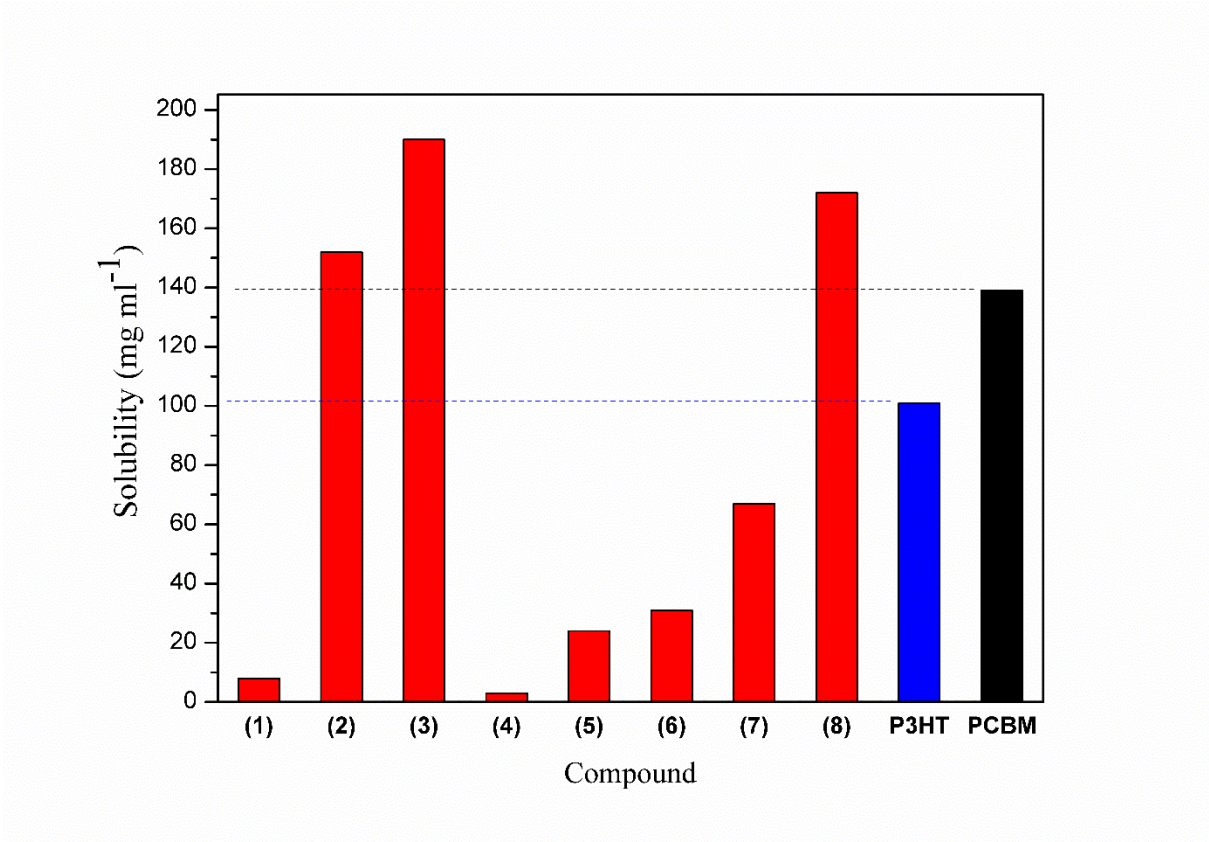

Figure 3. Solubility of different X_2-SiPcs, P3HT and PCBM in DCB.

Contact Angle

Contact angle measurements were carried out for X_2-SiPc, P3HT and $PC_{61}BM$ films, spincoated on octylctrichlorosilane (OTS) treated glass slides and the surface energy was estimated using the iterative Neumann's method [42]. The results are shown in Fig. 4. The X_2-SiPc films have intermediate surface energies to those of P3HT and $PC_{61}BM$. These results are in accordance with previous reports that found that X_2-SiPcs compatibilize the surface energy of P3HT and PCBM and tend to migrate to the

donor/acceptor interface [12]. The measured surface energy was also very similar for all X_2-SiPcs films (22.5 - 24.5 N mm^{-1}), which indicates that similar surface compatibilization effects can be expected when X_2-SiPcs are added to P3HT/PC_{61}BM BHJ. Previously[18] we have demonstrated via atomic force microscopy (AFM) that the addition of X_2-SiPcs (at concentrations relevant to the current study), does not lead to significant changes in P3HT/PC_{61}BM BHJ morphology. The discrepancy observed for compound (4) is attributed to bad film formation, resulting from its poor solubility (8 mg ml^{-1}) which led to nonhomogeneous films.

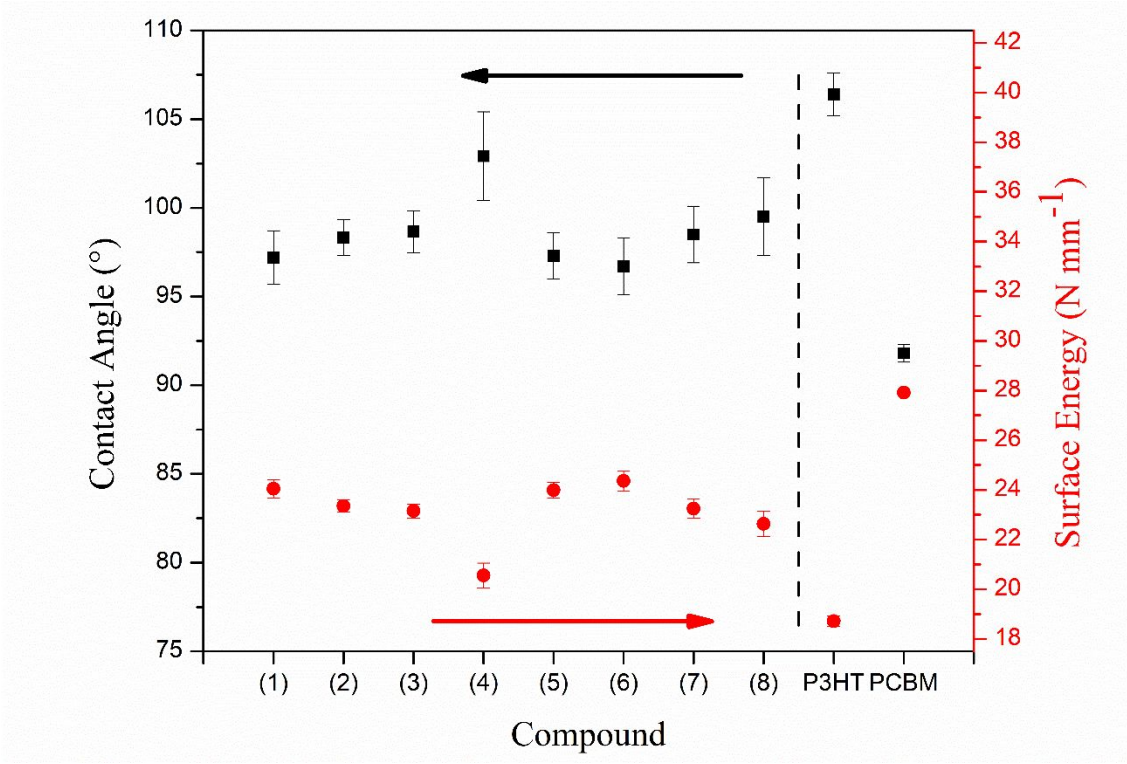

Figure 4. Contact angle and corresponding surface energy measurements of X_2-SiPc films on OTS treated glass

OPV performance

The eight X_2-SiPc derivatives were employed as ternary additives in P3HT/PC_{61}BM BHJ OPV devices in three different concentrations: 2.7 wt%, 3.7 wt% and 4.8 wt%. The results are presented on Table 2. The *Jsc* was measured by both current density vs. voltage (I-V) curves and EQE measurements. In general, *Jsc* values obtained with EQE are greater than those measured with the I-V curve. This is a common feature of thin-film devices due to photo current barrier effects.[43] Nevertheless, the difference is within 5-10%, which is consistent and acceptable for the purposes of this comparative work.

Table 2. Current density – voltage results for all the assembled OPVs and Jsc estimation from EQE measurements.

Compound	P3HT:PCBM:X_2-SiPc [a)]	*Voc* [b)]	*Jsc* [b)]	*Jsc* (EQE) [c)]	*FF* [b)]	PCE [b)]
Baseline	1:0.8:0	0.53 ± 0.00	-9.44 ± 0.31	10.33	0.54 ± 0.00	2.70 ± 0.07

	1:0.8:0.05	0.50 ± 0.01	-9.80 ± 0.75	9.84	0.48 ± 0.03	2.38 ± 0.37
(1)	1:0.8:0.07	0.51 ± 0.01	-9.18 ± 0.19	8.80	0.50 ± 0.02	2.37 ± 0.14
	1:0.8:0.09	0.52 ± 0.01	-9.34 ± 0.48	9.51	0.51 ± 0.02	2.50 ± 0.26
	1:0.8:0.05	0.53 ± 0.00	-10.35 ±0.34	11.49	0.56 ± 0.01	3.07 ± 0.09
(2)	1:0.8:0.07	0.54 ± 0.01	-10.62 ±0.28	11.81	0.57 ± 0.01	3.27 ± 0.08
	1:0.8:0.09	0.54 ± 0.01	-10.98 ± 0.27	11.76	0.56 ± 0.02	3.32 ± 0.12
	1:0.8:0.05	0.57 ± 0.01	-10.13 ± 0.30	12.07	0.59 ± 0.01	3.40 ± 0.12
(3)	1:0.8:0.07	0.54 ± 0.01	-10.32 ±0.22	11.73	0.57 ± 0.01	3.16 ± 0.05
	1:0.8:0.09	0.56 ± 0.01	-10.65 ± 0.41	11.69	0.57 ± 0.01	3.38 ± 0.09
	1:0.8:0.05	0.52 ± 0.00	-10.64 ± 0.29	12.79	0.50 ± 0.01	2.74 ± 0.10
(4)	1:0.8:0.07	0.53 ± 0.00	-11.00 ±0.29	11.60	0.53 ± 0.01	3.08 ± 0.11
	1:0.8:0.09	0.52 ± 0.01	-10.81 ± 0.27	11.14	0.51 ± 0.00	2.87 ± 0.13
	1:0.8:0.05	0.52 ± 0.00	-10.78 ± 0.33	12.16	0.53 ± 0.01	3.02 ± 0.11
(5)	1:0.8:0.07	0.54 ± 0.01	-10.78 ± 0.10	12.56	0.56 ± 0.02	3.24 ± 0.07
	1:0.8:0.09	0.54 ± 0.01	-10.71 ±0.28	12.00	0.56 ± 0.01	3.28 ± 0.08
	1:0.8:0.05	0.52 ± 0.00	-10.97 ± 0.27	10.97	0.54 ± 0.00	3.11 ± 0.06
(6)	1:0.8:0.07	0.54 ± 0.01	-10.51 ± 0.25	11.79	0.57 ± 0.01	3.27 ± 0.08
	1:0.8:0.09	0.56 ± 0.01	-10.65 ± 0.41	11.88	0.57 ± 0.01	3.38 ± 0.09
	1:0.8:0.05	0.55 ± 0.00	-10.12 ±0.23	11.10	0.57 ± 0.01	3.18 ± 0.08
(7)	1:0.8:0.07	0.55 ± 0.00	-10.80 ± 0.16	11.78	0.58 ± 0.01	3.43 ± 0.05
	1:0.8:0.09	0.56 ± 0.00	-10.55 ± 0.27	11.14	0.58 ± 0.01	3.43 ± 0.11
	1:0.8:0.05	0.55 ± 0.00	-9.75 ± 0.24	10.34	0.58 ± 0.01	3.13 ± 0.12
(8)	1:0.8:0.07	0.55 ± 0.00	-10.05 ± 0.24	10.96	0.59 ± 0.01	3.25 ± 0.12
	1:0.8:0.09	0.56 ± 0.00	-9.54 ± 0.16	10.63	0.58 ± 0.00	3.08 ± 0.07

[a]) Made with 20 mg ml^{-1} P3HT concentration, at 1000 RPM, dried in N_2 atmosphere, no annealing.

[b]) Measured from I-V curves, average of 5 devices, irradiation power of 1000 W m^{-2}.

[c]) Calculated by integrating the EQE spectra.

With the exception of compound (1), the inclusion of all the X_2-SiPcs improve the overall device performance, through increased *Jsc* and *FF*. *Jsc* is increased due to extended light harvesting at long wavelengths (>600 nm), which can be observed in the EQE spectra and overlaps with the absorption of SiPc chromophore (Fig. 2). The additives also effectively collect and transport charges at the P3HT and $PC_{61}BM$ interface, which causes the P3HT:$PC_{61}BM$ quantum efficiency contribution (300 nm to 600 nm) to increase as well. Fig. 5 displays the EQE spectra of every device listed on Table 2, where these features can be observed. In most devices, the X_2-SiPc EQE contribution (≈675 nm) is almost a perfect match to the absorption profile of X_2-SiPc in solution, which indicates little to no solid state aggregation of the X_2-SiPc,[44] further suggesting good dispersion of the SiPc derivative in the P3HT/$PC_{61}BM$ blend. We observed this type of behavior for all SiPc derivatives except for (4), (Figure 5d) the least soluble of the X_2-SiPc. At greater concentration of (4) we observe a red-shift and broadening of the EQE band, characteristic of solid-state interactions of SiPc aggregates. In fact, Honda *et al.*[12] demonstrated, through transient absorption spectroscopy, that bis(tri-n-hexylsilyl)-SiPc normally migrates to the amorphous P3HT/$PC_{61}BM$ interface, where its efficiency is greatest. Taking into consideration the

chemical similarities between all SiPc derivatives and the similar loading concentrations, we expect similar migration mechanism when blended in ternary films. We surmise the use of low solubility X_2-SiPcs as a ternary additive lead to poor OPV performance due to the formation of tertiary semicrystalline domains. These aggregates form a third independent phase that is not found at the P3HT and $PC_{61}BM$ interface and therefore disrupts efficient charge transfer, leading to no appreciable increase in EQE between 300 nm and 600 nm. While the devices containing compound (1) (second least soluble) do not show the same red-shift of the SiPc peak (Fig. 5a), a decrease in the P3HT/ $PC_{61}BM$ EQE contribution (300 nm to 600 nm) is observed, which indicates that the preferred morphology is also not achieved.

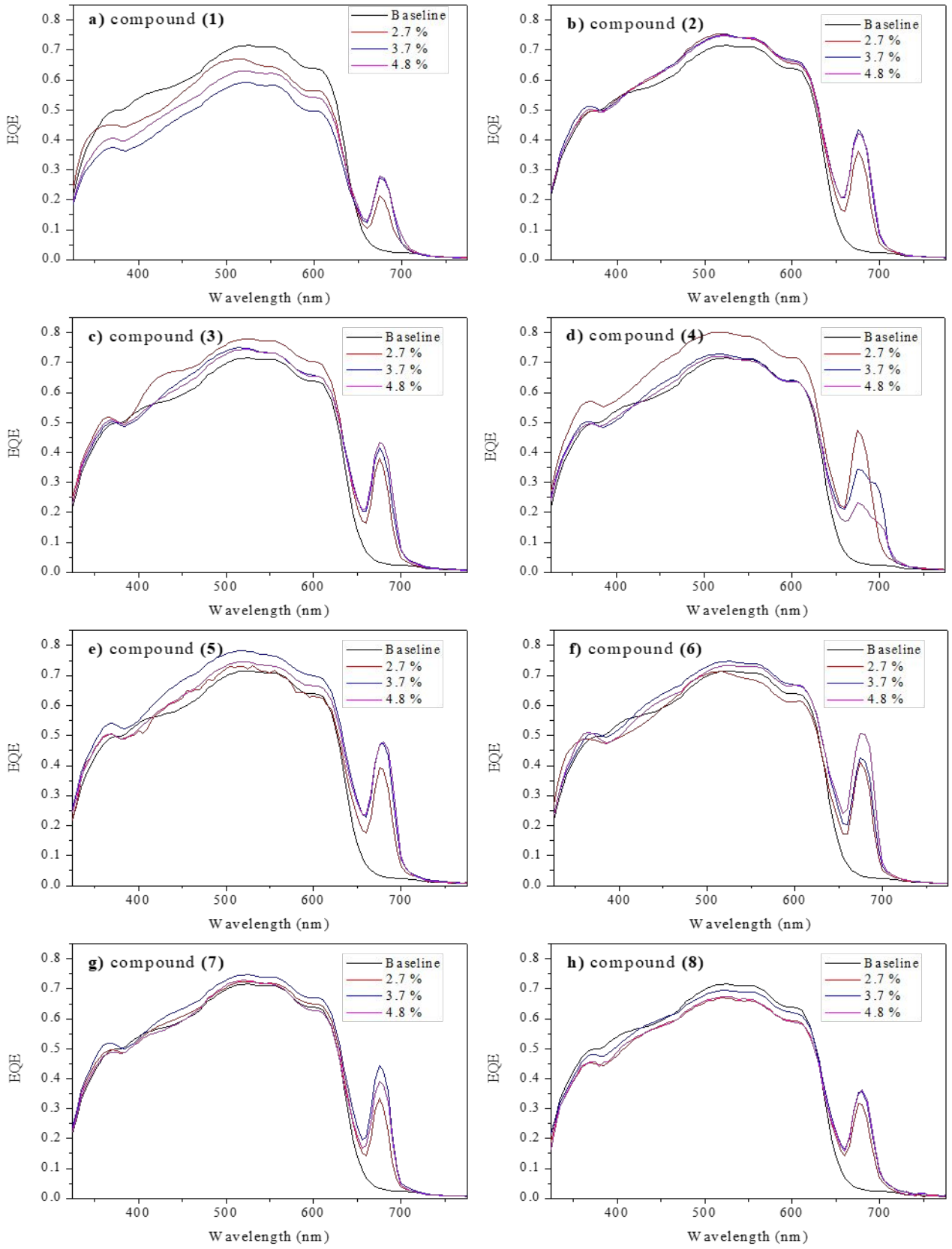
a) compound (1)
b) compound (2)
c) compound (3)
d) compound (4)
e) compound (5)
f) compound (6)
g) compound (7)
h) compound (8)
Baseline
2.7 %
3.7 %
4.8 %
EQE
Wavelength (nm)

Figure 5. EQE spectra of all the devices produced in the present worked divided by X_2-SiPc compounds.

In some instances, such as compounds (2) and (6), the greatest X_2-SiPc contribution to the photocurrent (e.g., EQE at 675 nm ≈ 42%) is achieved at the highest additive concentration (4.8%, pink line in Fig. 5b and 5f), but, overall, is approximately the same when compared to the medium concentration (3.7%, blue line Fig. 5). However, the best P3HT:PC_{61}BM photocurrent generation is observed at the 3.7% concentration, as it is the case for compounds (2), (5), (6), (7) and (8) (Fig 5b, 5e, 5f, 5g and 5h) that display up to 10% EQE increase in the 300 – 600nm region. At lower additive loading concentrations, not enough SiPc is located at the interface; however, at greater concentrations, it is expected that SiPc is located not only at the interface leading to trapped charges. Therefore, the 3.7% concentration is often the one with the highest efficiency because it maximizes the amount of SiPc at the interface without diffusing into the bulk of the film.

By simply changing the X_2-SiPc, which only differ in solubility, the overall BHJ OPV PCE varies from 2.4% to 3.4%, compared to PCE = 2.7% for the P3HT:PC_{61}BM baseline. Therefore, even though all the X_2-SiPc solubilities are above processability

range (minimum 8 mg ml^{-1}), the choice of additive can lead to improved or reduced OPV performance. Fig. 6 shows the correlation between solubility *PCE, Jsc, Voc* and fill factor, for the ternary BHJ OPV devices with the addition of 3.7 wt% X_2-SiPc.

The greatest PCE was obtained using compound (7), whose solubility is the closest to that of P3HT. We surmise this matching of solubility leads to more SiPc additive to be located at the donor:acceptor interface when the film dries. The same trend was found by Troshin *et al.*[38] where the authors reported that the best performance for P3HT/fullerene BHJ is achieved when the solubility of the donor/acceptor pair is similar, which leads to better nanomorphology. It would appear that in the case of the X_2-SiPcs, matching the solubility of P3HT has a stronger effect than matching $PC_{61}BM$'s solubilty. We expect this to be a result of X_2-SiPc's stronger interaction with P3HT than with $PC_{61}BM$ [12,22], i.e. they do not tend to solubilize in the $PC_{61}BM$ domains. Nonetheless, this is an area for further investigation.

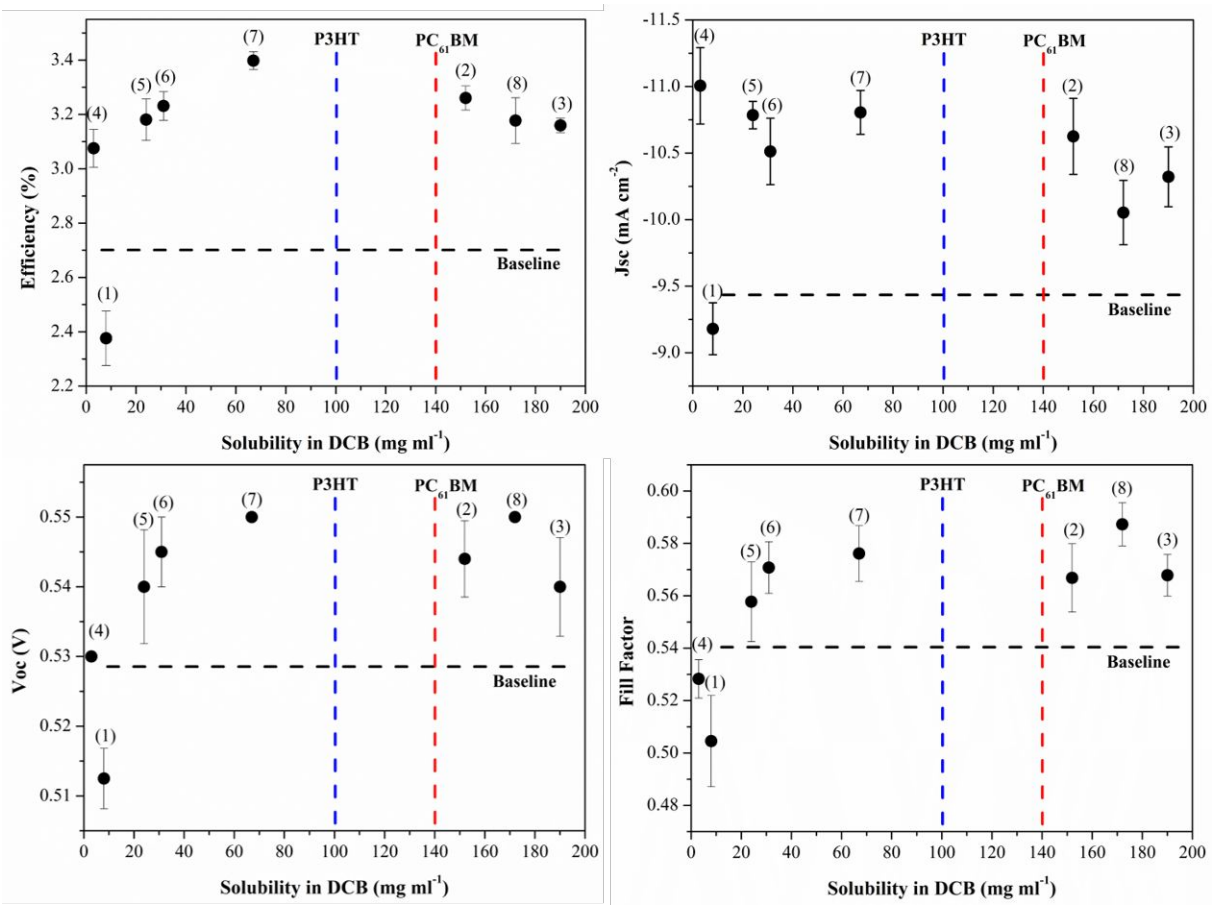

Figure 6. Solubility correlation with OPV performance parameters a) PCE, b) *Voc*, c) *Jsc* and d) Fill Factor.

The solubility of the X_2-SiPc ternary additive will determine the type of nanostructure formed during solvent evaporation, as a result of coprecipitation thermodynamics.[22,38] More specifically, a low solubility additive, such as (4) and (1), will tend to precipitate before P3HT and $PC_{61}BM$ and may be forced beyond the P3HT and $PC_{61}BM$ interface, or even form its own crystalline domains. When the solubility of the additives is similar or higher than that of the other components of the BHJ, the precipitation kinetic will

favor interfacial coverage. The proposed mechanism can be better visualized in Fig. 7. Honda *et al.*[12] found that the P3HT:$PC_{61}BM$ nanostructure is composed of relatively pure crystalline phases and an amorphous interfacial phase (Fig.7 a), and that the SiPcs performance is greatest when it is found at the amorphous interface where it can mediate the charge transfer between P3HT and $PC_{61}BM$, thereby contributing to the photogeneration of charges at higher wavelengths. Obviously, the concentration of X_2-SiPc additive will also play a role in the drying mechanics, as previously stated. A low additive concentration can prevent the scenario illustrated in Fig. 7 b) from happening; however, it will also limit the possible performance increase.

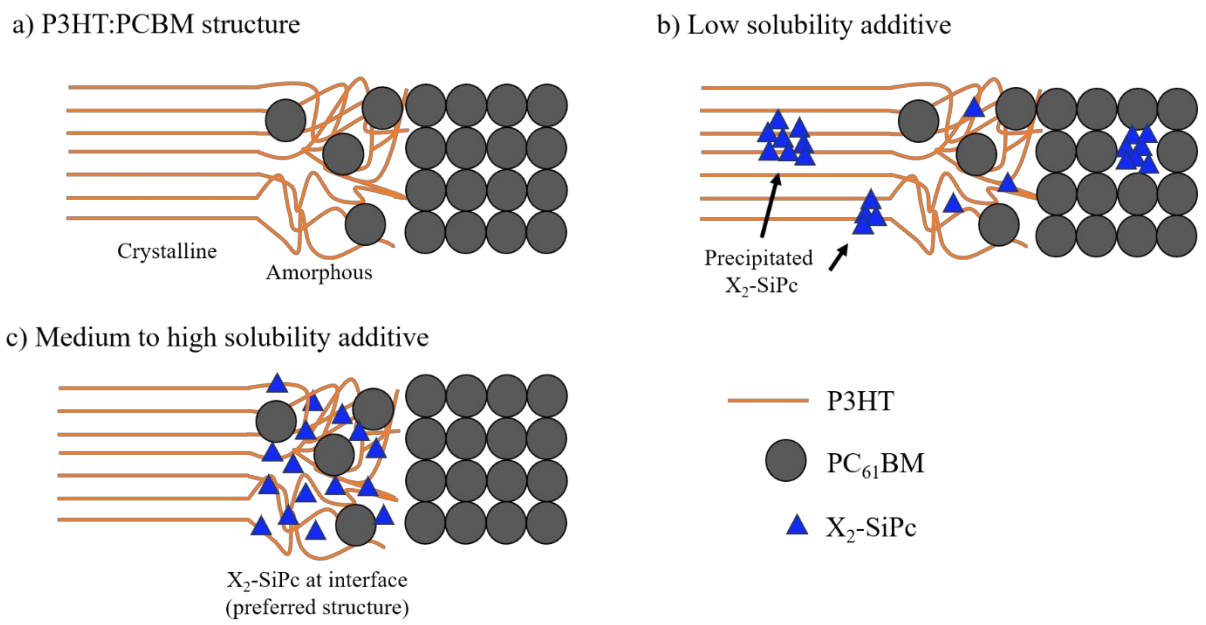

Figure 7. Proposed mechanism for the relationship found between additive and device performance: a) P3HT:PCBM structure when no additive is present; b) precipitation of low solubility X_2-SiPcs, with low chance of interfacial coverage and possible formation of crystalline domains; and c) Preferred configuration, which happens when the additive solubility somewhat matches that of the polymer donor (P3HT).

Whereas we could not identify any signs of crystallization in the high solubility X_2-SiPcs (2), (3) and (8), they demonstrate slightly lower performance than the additive (7), which indicates that an optimum window for additive solubility exists. This window is located near the solubility of the donor and acceptor materials. It is unclear why we observe a decrease in performance for the high solubility additives. It is possible that they tend to disperse in the P3HT phase, outside the interface. We have also observed that these compounds tend to dry slower and hold on to solvent molecules, which could happen during device fabrication, leading to some degree of charge trapping and slightly lower efficiency.

When we break down the PCE into its contributions, we can observe that both *Voc* and *Jsc* increases with solubility up to a point and then slightly decreases with increased solubility. The X_2-SiPcs located beyond the interface can act as charge

traps, given that their LUMO is lower than that of P3HT, which could lead to photogenerated electrons in P3HT transferring to the X_2-SiPc that is physically separated from PCBM. This leads to charge recombination and, consequently, a reduction in *Voc* and *Jsc*. The *FF* increases with solubility before reaching a plateau, which indicates a lower resistance across the film when the additive is more soluble. Overall, this study indicates that the solubility match between donor /acceptor phase and the ternary additive is critical for appropriate morphology and ultimately final device performance.

Conclusions

We successfully synthesized and characterized eight axially substituted SiPcs, which were then incorporated into P3HT:PCBM OPVs as ternary additives. The PCE of the devices varied from 2.4% to 3.4%, which represents up to 26% increase compared to the baseline (i.e., P3HT:PCBM OPVs with no ternary additives). Based on the results presented here, it is possible to conclude that changing the length of the axial alkylsilanes does not affect the energetics of the X_2-SiPcs, yet drastically influences the solubility. Furthermore, the solubility of the additive has a significant

effect on the performance of OPVs, with the best PCE achieved when the solubility of the X_2-SiPc is similar to that of P3HT, which favors the distribution of X_2-SiPcs at the P3HT:PCBM interface, where its effectiveness is greatest. While the interaction of X_2-SiPcs with the acceptor and donor pair also plays a role in the film nanomorphology and performance, we have shown that solubility is an important predictor of SiPcs performance as ternary additives. More research is needed to verify if this relationship is true for other ternary additives and donor:acceptor pairs, though we expect similar trends. Nevertheless, the relationship between performance and solubility can be an important tool for device engineering containing SiPcs.

Associated Content

The ^{1}HNMR and ^{13}CNMR spectra are available in supporting information file.

Ackknowledgements

The authors thank the University of Ottawa, the Canadian Foundation for Innovation (CFI), NSERC (RGPIN/ 2015-03987 and STPGP 506661-17) and T.M.G. is also grateful for the Ontario graduate student scholarship (OGS).

References

(1) Cai, W.; Gong, X.; Cao, Y. Polymer Solar Cells: Recent Development and Possible Routes for Improvement in the Performance. *Sol. Energy Mater. Sol. Cells* **2010**, *94* (2), 114–127. https://doi.org/10.1016/j.solmat.2009.10.005.

(2) You, J.; Dou, L.; Yoshimura, K.; Kato, T.; Ohya, K.; Moriarty, T.; Emery, K.; Chen, C.; Gao, J.; Li, G.; et al. A Polymer Tandem Solar Cell with 10.6% Power Conversion Efficiency. *Nat. Commun.* **2013**, *4*, 1410–1446. https://doi.org/10.1038/ncomms2411.

(3) Lipomi, D. J. Organic Photovoltaics: Focus on Its Strengths. *Joule* **2018**, *2* (2), 195–198. https://doi.org/10.1016/j.joule.2017.12.011.

(4) Fusella, M. A.; Lin, Y. L.; Rand, B. P. 20 - Organic Photovoltaics (OPVs): Device Physics. In *Handbook of Organic Materials for Electronic and Photonic Devices*; Elsevier Ltd., 2019; pp 665–693. https://doi.org/10.1016/B978-0-08-102284-9.00020-6.

(5) Yuan, J.; Zhang, Y.; Yuan, J.; Zhang, Y.; Zhou, L.; Zhang, G.; Yip, H.; Lau, T.; Lu, X. Single-Junction Organic Solar Cell with over 15 % Efficiency Using Fused-Ring Acceptor with Electron-Deficient Core Single-Junction Organic Solar Cell with over 15 % Efficiency Using Fused-Ring Acceptor with Electron-Deficient Core. *Joule* **2019**, *3*, 1–12. https://doi.org/10.1016/j.joule.2019.01.004.

(6) Cui, Y.; Yao, H.; Zhang, J.; Zhang, T.; Wang, Y.; Hong, L.; Xian, K.; Xu, B.; Zhang, S.; Peng, J.; et al. Over 16% Efficiency Organic Photovoltaic Cells Enabled by a Chlorinated Acceptor with Increased Open-Circuit Voltages. *Nat. Commun.* **2019**, *10* (1), 1–8. https://doi.org/10.1038/s41467-019-10351-5.

(7) Gambhir, A.; Sandwell, P.; Nelson, J. Solar Energy Materials & Solar Cells The Future Costs of OPV – A Bottom-up Model of Material and Manufacturing Costs with Uncertainty Analysis. *Sol. Energy Mater. Sol. Cells* **2016**, *156*, 49–58. https://doi.org/10.1016/j.solmat.2016.05.056.

(8) Goubard, F.; Wantz, G. Ternary Blends for Polymer Bulk Heterojunction Solar Cells. *Polym. Int* **2013**, *63* (July), 1362–1367. https://doi.org/10.1002/pi.4636.

(9) Lu, L.; Kelly, M. A.; You, W.; Yu, L. Status and Prospects for Ternary Organic Photovoltaics. *Nat. Photonics* **2015**, *9* (8), 491–500. https://doi.org/10.1038/nphoton.2015.128.

(10) Kipp, D.; Verduzco, R.; Ganesan, V. Block Copolymer Compatibilizers for Ternary Blend Polymer Bulk Heterojunction Solar Cells-an Opportunity for Computation Aided Molecular Design. *Molecular Systems Design and Engineering*. Royal Society of Chemistry 2016, pp 353–369. https://doi.org/10.1039/c6me00060f.

(11) Tsai, J. H.; Lai, Y. C.; Higashihara, T.; Lin, C. J.; Ueda, M.; Chen, W. C. Enhancement of P3HT/PCBM Photovoltaic Efficiency Using the Surfactant of Triblock Copolymer Containing Poly(3-Hexylthiophene) and Poly(4- Vinyltriphenylamine) Segments. *Macromolecules* **2010**, *43* (14), 6085–6091. https://doi.org/10.1021/ma1011182.

(12) Honda, S.; Yokoya, S.; Ohkita, H.; Benten, H.; Ito, S. Light-Harvesting Mechanism in Polymer/Fullerene/Dye Ternary Blends Studied by Transient Absorption Spectroscopy. *J. Phys. Chem. C* **2011**, *115* (22), 11306–11317. https://doi.org/10.1021/jp201742v.

(13) Grant, T. M.; Gorisse, T.; Dautel, O.; Wantz, G.; Lessard, B. H. Multifunctional Ternary Additive in Bulk Heterojunction OPV: Increased Device Performance and Stability. *J. Mater. Chem. A* **2017**, *5* (4), 1581–1587. https://doi.org/10.1039/C6TA08593H.

(14) Kim, H. J.; Han, A. R.; Cho, C. H.; Kang, H.; Cho, H. H.; Lee, M. Y.; Fréchet, J. M. J.; Oh, J. H.; Kim, B. J. Solvent-Resistant Organic Transistors and Thermally Stable Organic Photovoltaics Based on Cross-Linkable Conjugated Polymers. *Chem. Mater.* **2012**, *24* (1), 215–221. https://doi.org/10.1021/cm203058p.

(15) Claessens, C. G.; Hahn, U.; Torres, T. Phthalocyanines: From Outstanding Electronic Properties to

Emerging Applications. *Chem. Rec.* **2008**, *8* (2), 75–97. https://doi.org/10.1002/tcr.20139.

(16) Lessard, B. H.; White, R. T.; Al-Amar, M.; Plint, T.; Castrucci, J. S.; Josey, D. S.; Lu, Z. H.; Bender, T. P. Assessing the Potential Roles of Silicon and Germanium Phthalocyanines in Planar Heterojunction Organic Photovoltaic Devices and How Pentafluoro Phenoxylation Can Enhance π-π Interactions and Device Performance. *ACS Appl. Mater. Interfaces* **2015**, *7* (9), 5076–5088. https://doi.org/10.1021/am508491v.

(17) Yuen, A. P.; Jovanovic, S. M.; Hor, A. M.; Klenkler, R. A.; Devenyi, G. A.; Loutfy, R. O.; Preston, J. S. Photovoltaic Properties of M-Phthalocyanine/Fullerene Organic Solar Cells. *Sol. Energy* **2012**, *86* (6), 1683–1688. https://doi.org/10.1016/j.solener.2012.03.019.

(18) Dang, M.-T.; Grant, T. M.; Yan, H.; Seferos, D. S.; Lessard, B. H.; Bender, T. P.; Miller, J. a.; Goethem, E. M. Van; Kenney, M. E.; Lu, Z.-H. Bis(Tri-n-Alkylsilyl Oxide) Silicon Phthalocyanines: A Start to Establishing a Structure Property Relationship as Both Ternary Additives and Non-Fullerene Electron Acceptors in Bulk Heterojunction Organic Photovoltaic Devices. *J. Mater. Chem. A* **2017**, *126*, 3378–3379. https://doi.org/10.1039/C6TA10739G.

(19) Grant, T. M.; Rice, N. A.; Muccioli, L.; Castet, F.; Lessard, B. H. Solution-Processable n-Type Tin Phthalocyanines in Organic Thin Film Transistors and as Ternary Additives in Organic Photovoltaics. *ACS Appl. Electron. Mater.* **2019**, *1* (4), 494–504. https://doi.org/10.1021/acsaelm.8b00113.

(20) Honda, S.; Ohkita, H.; Benten, H.; Ito, S. Multi-Colored Dye Sensitization of Polymer/Fullerene Bulk Heterojunction Solar Cells. *Chem. Commun.* **2010**, *46* (35), 6596–6598. https://doi.org/10.1039/c0cc01787f.

(21) Honda, S.; Nogami, T.; Ohkita, H.; Benten, H.; Ito, S. Improvement of the Light-Harvesting Efficiency in Polymer/Fullerene Bulk Heterojunction Solar Cells by Interfacial Dye Modification. *ACS Appl. Mater. Interfaces* **2009**, *1* (4), 804–810. https://doi.org/10.1021/am800229p.

(22) Honda, S.; Ohkita, H.; Benten, H.; Ito, S. Selective Dye Loading at the Heterojunction in Polymer/Fullerene Solar Cells. *Adv. Energy Mater.* **2011**, *1* (4), 588–598. https://doi.org/10.1002/aenm.201100094.

(23) Lim, B.; Bloking, J. T.; Ponec, A.; McGehee, M. D.; Sellinger, A. Ternary Bulk Heterojunction Solar Cells: Addition of Soluble NIR Dyes for Photocurrent Generation beyond 800 Nm. *ACS Appl. Mater. Interfaces* **2014**, *6* (9), 6905–6913. https://doi.org/10.1021/am5007172.

(24) Ke, L.; Min, J.; Adam, M.; Gasparini, N.; Hou, Y.; Perea, J. D.; Chen, W.; Zhang, H.; Fladischer, S.; Sale, A.-C.; et al. A Series of Pyrene-Substituted Silicon Phthalocyanines as Near-IR Sensitizers in Organic Ternary Solar Cells. *Adv. Energy Mater.* **2016**, *6* (7), 1502355. https://doi.org/10.1002/aenm.201502355.

(25) Ke, L.; Gasparini, N.; Min, J.; Zhang, H.; Adam, M.; Rechberger, S.; Forberich, K.; Zhang, C.; Spiecker, E.; Tykwinski, R. R.; et al. Panchromatic Ternary/Quaternary Polymer/Fullerene BHJ Solar Cells Based on Novel Silicon Naphthalocyanine and Silicon Phthalocyanine Dye Sensitizers. *J. Mater. Chem. A* **2017**, *5* (6), 2550–2562. https://doi.org/10.1039/C6TA08729A.

(26) Zysman-Colman, E.; Ghosh, S. S.; Xie, G.; Varghese, S.; Chowdhury, M.; Sharma, N.; Cordes, D. B.; Slawin, A. M. Z.; Samuel, I. D. W. Solution-Processable Silicon Phthalocyanines in Electroluminescent and Photovoltaic Devices. *ACS Appl. Mater. Interfaces* **2016**, *8* (14), 9247–9253. https://doi.org/10.1021/acsami.5b12408.

(27) Pearson, A. J.; Plint, T.; Jones, S. T. E.; Lessard, B. H.; Credgington, D.; Bender, T. P.; Greenham, N. C. Silicon Phthalocyanines as Dopant Red Emitters for Efficient Solution Processed OLEDs. *J. Mater. Chem. C* **2017**, *5* (48), 12688–12698. https://doi.org/10.1039/c7tc03946h.

(28) Plint, T.; Lessard, B. H.; Bender, T. P. Assessing the Potential of Group 13 and 14 Metal/Metalloid Phthalocyanines as Hole Transport Layers in Organic Light Emitting Diodes. *J. Appl. Phys.* **2016**, *119* (14), 1455021–1455029. https://doi.org/10.1063/1.4945377.

(29) Melville, O. A.; Lessard, B. H.; Bender, T. P. Phthalocyanine-Based Organic Thin-Film Transistors: A Review of Recent Advances. *ACS Appl. Mater. Interfaces* **2015**, *7* (24), 13105–13118. https://doi.org/10.1021/acsami.5b01718.

(30) Melville, O. A.; Grant, T. M.; Mirka, B.; Boileau, N. T.; Park, J.; Lessard, B. H. Ambipolarity and Air Stability of Silicon Phthalocyanine Organic Thin-Film Transistors. *Adv. Electron. Mater.* **2019**, *5* (1900087), 1–7. https://doi.org/10.1002/aelm.201900087.

(31) Melville, O. A.; Grant, T. M.; Lessard, B. H. Silicon Phthalocyanines as N-Type Semiconductors in Organic Thin Film Transistors. *J. Mater. Chem. C* **2018**, *6* (20), 5482–5488. https://doi.org/10.1039/c8tc01116h.

(32) Yutronkie, N. J.; Grant, T. M.; Melville, O. A.; Lessard, B. H.; Brusso, J. L. Old Molecule, New Chemistry: Exploring Silicon Phthalocyanines as Emerging N-Type Materials in Organic Electronics. *Materials (Basel)*. **2019**, *12* (8), 5–10. https://doi.org/10.3390/ma12081334.

(33) Grant, T. M.; Rice, N. A.; Muccioli, L.; Castet, F.; Lessard, B. H. Solution-Processable n-Type Tin Phthalocyanines in Organic Thin Film Transistors and as Ternary Additives in Organic Photovoltaics. *ACS*

Appl. Electron. Mater. **2019**, *1* (4), 494–504. https://doi.org/10.1021/acsaelm.8b00113.

(34) Xue, Z.; Wang, S.; Yang, J.; Zhong, Y.; Qian, M.; Li, C.; Zhang, Z.; Xing, G.; Huettner, S.; Tao, Y.; et al. Enhanced Power Conversion Efficiency in Iridium Complex-Based Terpolymers for Polymer Solar Cells. *npj Flex. Electron.* **2018**, *2* (1), 1–7. https://doi.org/10.1038/s41528-017-0014-9.

(35) Lessard, B. H.; Grant, T. M.; White, R.; Thibau, E.; Lu, Z.-H.; Bender, T. P. The Position and Frequency of Fluorine Atoms Changes the Electron Donor/Acceptor Properties of Fluorophenoxy Silicon Phthalocyanines within Organic Photovoltaic Devices. *J. Mater. Chem. A* **2015**, *3* (48), 24512–24524. https://doi.org/10.1039/C5TA07173A.

(36) MacHui, F.; Langner, S.; Zhu, X.; Abbott, S.; Brabec, C. J. Determination of the P3HT:PCBM Solubility Parameters via a Binary Solvent Gradient Method: Impact of Solubility on the Photovoltaic Performance. *Sol. Energy Mater. Sol. Cells* **2012**, *100*, 138–146. https://doi.org/10.1016/j.solmat.2012.01.005.

(37) Berriman, G. A.; Holmes, N. P.; Holdsworth, J. L.; Zhou, X.; Belcher, W. J.; Dastoor, P. C. A New Model for PCBM Phase Segregation in P3HT:PCBM Blends. *Org. Electron. physics, Mater. Appl.* **2016**, *30*, 12–17. https://doi.org/10.1016/j.orgel.2015.12.014.

(38) Troshin, P. A.; Hoppe, H.; Renz, J.; Egginger, M.; Mayorova, J. Y.; Goryachev, A. E.; Peregudov, A. S.; Lyubovskaya, R. N.; Gobsch, G.; Sariciftci, N. S.; et al. Material Solubility-Photovoltaic Performance Relationship in the Design of Novel Fullerene Derivatives for Bulk Heterojunction Solar Cells. *Adv. Funct. Mater.* **2009**, *19* (5), 779–788. https://doi.org/10.1002/adfm.200801189.

(39) Lowbry, M. K.; Starshak, A. J.; John, S. J.; Esposito, N.; Krueger, P. C.; Kenney, M. E. DichloroCphthalocyaninoJsilicon. *Inorg. Chem.* **1965**, *4* (1), 128. https://doi.org/10.1021/ic50023a036.

(40) Gessner, T.; Sens, R.; Ahlers, W.; Vamvakaris, C. Preparation of Silicon Phthalocyanines and Germanium Phthalocyanines and Related Substances. *US 2010/0113767* **2010**.

(41) Sauer, N. N. Green Chemistry: Frontiers in Benign Chemical Syntheses and Processes Edited by Paul T. Anastas and Tracy C. Williamson (U. S. Environmental Protection Agency). Oxford University Press: New York, NY. 1999. 360 Pp. $115.00. ISBN 0-19-850170-6. *J. Am. Chem. Soc.* **2000**, *122* (22), 5419–5420. https://doi.org/10.1021/ja995756g.

(42) Li, D.; Neumann, A. W. A Reformulation of the Equation of State for Interfacial Tensions. *J. Colloid Interface Sci.* **1990**, *137* (1), 1–4.

(43) Scheer, R.; Schock, H. W. *Chalcogenide Photovoltaics: Physics, Technologies, and Thin Film Devices*; 2011. https://doi.org/10.1002/9783527633708.

(44) Lessard, B. H.; Dang, J. D.; Grant, T. M.; Gao, D.; Seferos, D. S.; Bender, T. P. Bis(Tri- n -Hexylsilyl Oxide) Silicon Phthalocyanine: A Unique Additive in Ternary Bulk Heterojunction Organic Photovoltaic Devices. *ACS Appl. Mater. Interfaces* **2014**, *6* (17), 15040–15051. https://doi.org/10.1021/am503038t.

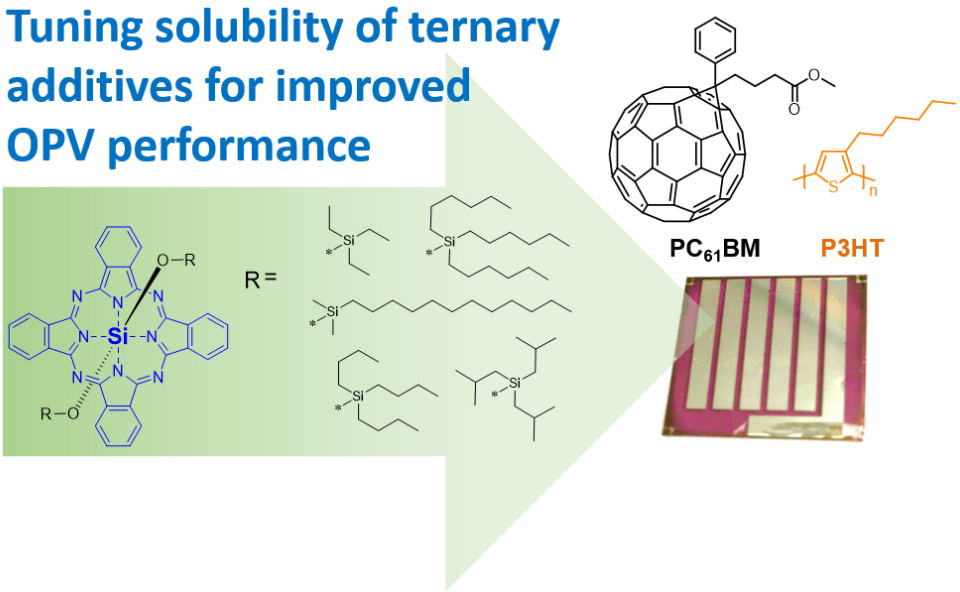

TOC

170x105mm (150 x 150 DPI)